Theoretical study of iron-filled carbon nanotubes

Mariana Weissmann,[1] Griselda García,[2] Miguel Kiwi,[2] Ricardo Ramírez,[2] and Chu-Chun Fu[3]
[1]*Departamento de Física, Comisión Nacional de Energía Atómica, Avenida del Libertador 8250, (1429) Buenos Aires, Argentina*
[2]*Facultad de Física, Universidad Católica de Chile, Casilla 306, Santiago, Chile 6904411*
[3]*Service de Recherches de Metallurgie Physique, CEA/Saclay, 91191 Gyf-sur-Yvette, Cedex, France*
(Received 12 October 2005; revised manuscript received 25 January 2006; published 28 March 2006)

The structural arrangements and magnetic properties of iron encapsulated in single wall carbon nanotubes (SWCNT) are investigated. Fe nanowires are of interest because of their potential use in spintronics. They have also been fabricated inside carbon nanotubes, where occasionally exchange bias has also been detected. An additional motivation to study these systems is to contribute to the understanding of how the iron-carbon interaction determines the magnetic ordering. Here we investigate, using *ab initio* methods, the geometry and magnetic structure of freestanding and encapsulated Fe nanowires, and also the properties of the nanowire-nanotube system when defects are present in the single wall carbon nanotube. When the ratio of the nanowire to nanotube diameter is small the system is stable and the spin polarization at the Fermi energy is large, thus making the system potentially interesting for spintronics. When this ratio is close to one the system is less stable and a tendency towards antiferromagnetic ordering is observed.

DOI: 10.1103/PhysRevB.73.125435 PACS number(s): 71.10.−w, 71.20.Tx, 72.80.Le

I. INTRODUCTION

For some time research in the field of carbon nanotubes (CNT) has attracted a great deal of interest.[1] In particular, the filling of these nanotubes with magnetic elements, like iron or other transition metals, makes them potential candidates for use in nanodevices and in the magnetic storage industry.[2,3] Their possible use is suggested by at least two features they may display: strong differences between majority and minority densities of states at the Fermi level[4] and the experimental observation of exchange bias that was recently reported.[5,6] Moreover, the possibility of generating spin polarization in a nanotube in contact with a magnetic substrate has also been examined recently.[7] On the experimental front CNT have been successfully filled with several metals.[8] In addition, metallic nanotubes and nanowires[9] have also been fabricated and investigated theoretically.[10,11] These developments open a new and promising field, which is just beginning to be explored. However, not all the experimental and theoretical papers report the same properties.[12–14] In fact, these properties depend on the theoretical approaches that are adopted, the techniques with which they are treated, as well as the fabrication procedures of the samples.

This paper, as other previous work,[4,15–19] attempts to develop a better understanding of the interaction between metal nanowires and carbon coatings. Our first step in this direction was to investigate freestanding Fe nanowires, focusing our interest on hcp (0001) and bcc (011) wire structures since they are the ones that, along the nanowire axis, have a periodicity that is compatible with both the CNT periodicity and the requirement that the unit cell be small enough to carry out meaningful calculations within reasonable computing time. Thus we discarded, for the time being, Fe-fcc structures since to allow for the compatibility of the nanowire and CNT periodicities a rather large unit cell is required.

We started carrying out *ab initio* calculations for hcp bulk iron. While the antiferromagnetic (AF) bulk hcp structure converges well with both codes used in this paper (Wien2k and SIESTA) neither achieved convergence for the ferromagnetic (FM) iron hcp bulk structure. However, when the same codes were implemented for nanowires along the hcp (0001) direction, the resulting minimum energy magnetic structure is FM. Moreover, as will be discussed below, for an increasing number of atoms per layer the FM and the antiparallel (AP) ordering, in which two successive layers have opposite magnetizations, have almost identical energies. FM order finally sets in because it achieves a larger energy gain than the AP when both of them are allowed to relax. This naturally leads to the conjecture that when the nanowire is encapsulated by a CNT, AP order may stabilize, since the CNT is quite rigid and acts as a containing wall.

On the other hand, if the FM and the AP structures are very close in energy it is quite likely that they may coexist. In turn, this coexistence could generate the exchange bias phenomenon,[20,21] which has been suggested by experiment,[5] thus opening the way to uses of interest to novel technologies.[22,23]

II. CALCULATION METHODS

For the calculations we used mainly SIESTA,[24–26] but also the Wien2k code[27] which we employed previously.[4] This way we are in a position to compare and check results. The Wien2k code is an implementation of the full potential linear augmented plane waves (FPLAPW) method. We used a spin polarized approach and the exchange and correlation given by Perdew, Burke, and Ernzerhoff.[28–30] The generalized gradient approximation (GGA) was chosen because it gives good results for the bulk bcc Fe lattice parameter and cohesive energy. The number of plane waves used, given by the parameter RKM=7, corresponds to an energy cutoff of 15 Ry. The calculation is scalar relativistic and includes local orbitals for the 3*p* states of Fe. The atomic sphere radii (muffin tins) were taken as 2 (a.u.) for Fe and 1.8 (a.u.) for C.

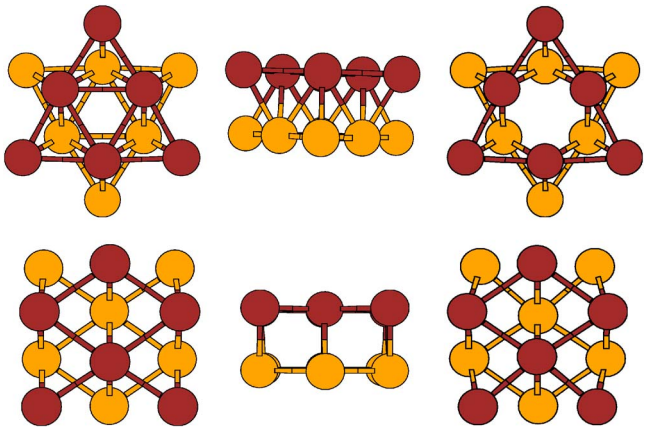

FIG. 1. (Color online) Nanowires with 6 Fe atoms per layer arranged in two crystal structures, hcp (0001) and bcc (110), are illustrated in the top and bottom panels, respectively. The top and lateral view of the initial, or unrelaxed, system is on the left and the top view of the relaxed structure is on the right. The darker and lighter circles correspond to the different layers in the unit cell.

For the relaxation of the structures we found it more convenient to use the Siesta code,[24–26] which is also a DFT code[31,32] but replaces the core electrons by nonlocal norm-conserving pseudopotentials and describes the valence electrons by a linear combination of numerical pseudoatomic orbitals. The pseudopotential and the basis set for Fe atoms are the same as in Fu *et al.*[33,34] The cutoff radius for the pseudopotential of C is set to 0.66 Å, and its basis set consists of localized functions with a cutoff radius of 2.22 Å for the two functions, and 2.64 Å for the six functions representing, respectively, the 2*s* and the 2*p* states. The 3*d* state is included as polarized orbitals in order to increase angular flexibility. The charge density is represented on a regular real space grid of 2400 points/Å^3. Relaxation of the structure by the conjugate gradient method was performed until the forces on each atom were less than 0.04 eV/Å. A large number of *k* points along the periodic axis was used for bare nanowires, but for the encapsulated ones the unit cell contains many more atoms, so that only a few *k* points were calculated. In our previous paper[4] we used the Wien code without relaxing the geometries, but in the present calculations we use larger unit cells, of up to 60 atoms, and structural relaxation. For this purpose the Siesta code is more convenient and faster. We therefore recalculated the bare Fe wires, and also a few systems containing both C and Fe atoms, verifying that the agreement is excellent, as will be shown below.

III. MODEL GEOMETRIES AND RESULTS

A. Free standing Fe nanowires

To make significant comparisons we start by considering free standing iron nanowires. Two structures were adopted: the Fe hcp (0001) and the Fe bcc (110) crystal structures illustrated in Fig. 1. For them we adopted a unit cell size, along the tube axis, of 4.06 Å, which is the experimental separation between layers in fcc and hcp iron along the (111) direction and also that between layers in bcc iron along the (110) direction. All the results we report in this contribution are obtained without relaxing the cell in the axis direction.

For hcp (0001) iron nanowires we computed configurations with 3, 6, 12, and 18 atoms per layer, both ordered FM and AP. Instead, for the bcc (110) iron case only FM ordered wires were considered. The bcc (110) iron nanowire is a cylindrical cut of iron bcc, that repeats periodically along the wire axis. We consider bilayers of 9 (4+5), 11 (5+6), 12 (6+6), 20 (10+10), 24 (12+12), and 27 (13+14) atoms, where the number of Fe atoms in each of the two layers of the bilayer is indicated in parentheses.

The differences between the cohesive energy of Fe in hcp (0001) nanowires (NW), and that of bulk bcc Fe obtained with the same type of calculation, ΔE_{NW}, are given in Table I. Analytically they are given by

$$\Delta E_{\mathrm{NW}} = \frac{E_{\mathrm{NW}}}{N_{\mathrm{Fe}}} - E_B, \tag{1}$$

where E_{NW} is the total energy of the unit cell containing N_{Fe} iron atoms. Our calculations yield for bulk bcc iron a cohesive energy of E_B=6.5 eV/atom. It is clear from Table I that FM order is always favorable, since for the nanowires $\Delta E^R_{\mathrm{AP}} > \Delta E^R_{\mathrm{FM}}$, and we also find that the nanowire is stable against dissociation into atoms. The relaxation of the structure to minimize its energy, which implies an increase of the wire diameter, is seen to be more important in the FM cases.

The particular case of 6 Fe atoms per layer was also calculated with the Wien2k code, both for the unrelaxed and the relaxed configurations. The ferromagnetic configuration is also preferred and the difference between FM and AP ener-

TABLE I. Energy differences per atom, relative to bulk bcc Fe for freestanding hcp (0001) iron nanowires of *N* atoms per layer, or 2*N* per unit cell. *NR* stands for unrelaxed and *R* for relaxed. FM stands for ferromagnetic and AP for antiparallel alignment. NC denotes nonconvergence of the calculation. The magnetic moments μ_{at} of the peripheral (*P*) and interior (*I*) Fe atoms are also shown.

N	$\Delta E^{NR}_{\mathrm{FM}}$ (eV)	$\Delta E^{R}_{\mathrm{FM}}$ (eV)	$\Delta E^{NR}_{\mathrm{AP}}$ (eV)	$\Delta E^{R}_{\mathrm{AP}}$ (eV)	μ^{P}_{at} (μ_B)	μ^{I}_{at} (μ_B)
3	1.86	1.84	2.02	2.01	3.0	3.0
6	1.54	1.48	1.64	1.61	3.2	2.6
12	1.06	0.99	1.07	1.04	2.9	2.6
18	0.97	0.89	0.99	0.97	3.1	2.5
∞	NC	0.04	NC	0.02		

TABLE II. Per atom energy differences, relative to the Fe bcc bulk value, for FM ordered bcc (110) iron nanowires. Here, in contrast with Table I, N is number of atoms per bilayer. NR and R stand for relaxed and unrelaxed, respectively. The magnetic moments μ_{at} of the peripheral (P) and interior (I) Fe atoms are also shown.

N	ΔE_{FM}^{NR} (eV)	ΔE_{FM}^{R} (eV)	μ_{at}^{P} (μ_B)	μ_{at}^{I} (μ_B)
9	1.60	1.54	3.0	2.1
11	1.58	1.51	3.1	2.3
12	1.35	1.31	3.0	2.5
20	1.01	0.98	3.0	2.5
24	0.91	0.89	3.0	2.5
27	0.91	0.87	3.0	2.5

gies is 0.09 eV for the unrelaxed case, the magnetic moments being 2.5 and 3.0 μ_B for the internal and peripheral atoms, respectively. The energy difference between the relaxed and unrelaxed ferromagnetic cases is 0.7 eV, very close to that obtained with the Siesta code.

In Table II we provide the energy differences for bcc (110) FM iron nanowires, relative to the bulk value. Comparison of the rows corresponding to $N=12$ of Tables I and II shows a slight preference for the bcc structure. However, the difference is small enough to conjecture that encapsulating these nanowires in a CNT might change the outcome and allow for metastable coexistence of hcp/bcc, or eventually even fcc/bcc, arrangements. We mention that the interlayer separation of hcp (0001) and bcc (110) is identical if the nearest-neighbor distance is kept constant.

B. Fe nanowires encapsulated in SWCNT

To integrate this study with our previous work on carbon coated nanowires[4] we recalculated the same structures with the SIESTA code. The purpose is twofold: to confirm consistency between the methods, and to study the relaxation of the geometrical structures. We found that the lowest energy configuration is also AP and that the energy difference between FM and AP alignment is also of the order of 0.01 eV per atom. The magnetic moments and the charge transfers are also very similar. However, when the structure is allowed to relax the geometry changes significantly, the carbon atoms move towards the axis and intercalate with the peripheral irons. Again the lowest energy configuration is AP, but the interior Fe atoms carry a lower magnetic moment than the peripheral ones, contrary to what happened in the unrelaxed case. The large changes due to relaxation are a consequence of the low coordination of C atoms in these systems. We do not expect this to carry on to iron encapsulated in carbon nanotubes, since in that case the covalency between Fe and C is much smaller.

Now we specify the structure of the iron wires encapsulated in single wall carbon nanotubes (SWCNT). It is important to keep in mind that the Fe wire and the SWCNT must share a unit cell of reasonable size, which is repeated periodically along the system axis, with a misfit of only a few

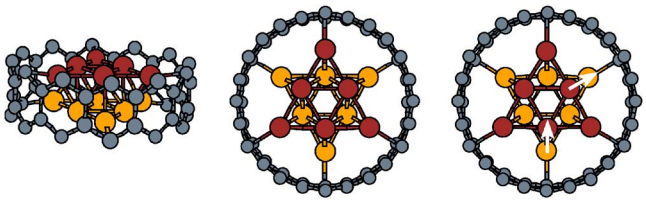

FIG. 2. (Color online) Iron hcp (0001) nanowire, with 6 atoms per layer, encapsulated in a carbon (12,0) zig-zag nanotube. The smaller peripheral atoms depict carbon, the larger interior atoms depict Fe, darker and lighter ones correspond to the different layers in the unit cell. We show the initial or unrelaxed system, in top and lateral viewpoints on the left and the top view of the relaxed structure on the right. The arrows indicate the direction of displacement of the atoms as the system relaxes.

percent. The fact that the hcp (0001) structure can be obtained with a two iron layer unit cell that is compatible with the periodicity of the SWCNT, and the fact that the hcp structure could give an AP solution, are the reasons to justify the calculation using wires with hcp structure. On the other hand, the fcc iron structure has a minimal three layer unit cell and to fit it to the nanotube periodicity at least six layers are required. For the bare SWCNT, and also for the encapsulated iron cases, we adopted the experimental distance of 4.26 Å, which implies a misfit of around 5% with the previous unit cell of the bare Fe nanowires. We have verified that Fe nanowires calculated with an expanded unit cell of 4.26 Å do not change appreciably their electronic or magnetic properties.

For the SWCNT we have chosen the zig-zag structures denoted[35] as $(n,0)$. In particular, we limit our attention to nanotubes with $9 \leqslant n \leqslant 15$. An illustration of the (12,0) case is given in Fig. 2.

We have considered the following arrangements:

(1) Encapsulated Fe hcp (0001) wires of 6 atoms per layer in zig-zag nanotubes $(n,0)$ with n ranging from 9 to 15.

(2) Encapsulated Fe bcc(110) wires of 6 atoms per layer in zig-zag nanotubes (12,0).

(3) Encapsulated Fe hcp (0001) wires, with 12 atoms per layer, in (13,0) and (15,0) carbon nanotubes.

Our strategy is to keep the NW structure fixed (6 and 12 Fe per layer) and vary the value of n of the SWCNT to study the effects of encapsulation on the electronic and magnetic properties of the composite system.

In order to determine the stability of iron encapsulated in the various SWCNT that are studied, we calculate the interaction energies E by subtracting the energy of the bare SWCNT plus that of the free standing relaxed Fe nanowire from the energy of the (CNT+Fe) system, that is $E = E_{CNT+Fe} - E_{CNT} - E_{NW}$. For the calculation of these encapsulated cases we use the unit cell size of the bare SWCNT, assuming that the strong bonding of the nanotube prevails. We have confirmed this for one particular case, by allowing the cell size to relax along the wire axis. The results are displayed in Table III. For the six iron per layer wire, in the hcp (0001) structure, the (12,0), (13,0), and (15,0) encapsulated systems are attractive and FM. Relaxation of the structures increases slightly the diameter of the SWCNT and the Fe atoms move away from C and closer to each other. This is

TABLE III. Interaction energies E, magnetic moments μ_{at}, and electronic charges q, of Fe encapsulated in $(n,0)$ single wall carbon nanotubes. *NR* indicates nonrelaxed and *R* relaxed systems. $\Delta E = E^{R}_{CNT+Fe} - E^{NR}_{CNT+Fe}$. The superindices *P* and *I* stand for peripheral and interior iron atoms, respectively. The last two rows show the results for free standing iron wires with 6 and 12 atoms per layer, for comparison.

Type	E^{NR} (eV)	E^{R} (eV)	ΔE (eV)	μ^{P}_{at} (μ_B)	μ^{I}_{at} (μ_B)	q^P	q^I
(9,0)-6Fe	332.0	13.9	−318.1	0.4	1.9	7.95	7.98
(10,0)-6Fe	115.9	5.6	−110.3	1.9	2.2	7.95	8.00
(11,0)-6Fe	19.4	−3.8	−23.2	2.6	2.6	8.00	8.00
(12,0)-6Fe	−1.4	−4.3	−2.9	2.7	2.7	8.00	8.00
(13,0)-6Fe	−3.6	−4.6	−1.0	2.9	2.7	7.99	8.01
(15,0)-6Fe	−1.9	−2.4	−0.5	3.2	2.7	8.01	7.97
(13,0)-12Fe	91.9	2.4	−89.5	−1.1	2.1	7.95	7.98
(15,0)-12Fe	−2.4	−6.9	−4.5	2.8	2.6	7.99	8.00
6Fe				3.2	2.6	8.05	7.95
12Fe				2.9	2.6	7.98	8.02

shown in Fig. 2 using arrows to indicate the displacements of the Fe atoms. For the (11,0) system the relaxed encapsulated structure is attractive, but the unrelaxed one is repulsive. For thinner SWCNT the interaction is repulsive, but relaxation of the structure decreases considerably to this repulsion. We remark that the initial configuration chosen is arbitrary, as the Fe wire may be rotated with respect to the SWCNT which, if the Fe and C atoms are close, may change the interaction energy and even the magnetic configuration. In fact, for the (9,0) case we found two possible relaxed structures depending on the initial configuration. One is stabilized as FM, although the magnetic moments of the Fe atoms close to C are very small, while the other is AP.

The general tendency is that the encapsulated nanowires are stable and FM unless the Fe atoms are positioned too close to the carbons, at which point the system becomes unstable and the AP structure may be preferred. In many cases both FM and AP structures could be stabilized as the energy difference between them was small. Thus, one could expect them to coexist at finite temperatures, with the implications for the exchange bias phenomenon[5,20,21] we mentioned before.

Apart from hcp (0001) encapsulated wires we also computed the energies and magnetic moments of an iron bcc (110) nanowire of 6 Fe atoms per layer, in the FM structure, encapsulated in a (12,0) SWCNT. The magnetic moment is 2.6 μ_B per iron atom. The energy of this system is only 0.1 eV per Fe atom lower than that of the hcp (0001) nanowire with 6 Fe atoms per layer. The AP solution was also found but it has a much larger energy.

For the 12-Fe per layer wires we studied only two encapsulated cases, in (13,0) and (15,0) SWCNT; the larger diameter (15,0) case turns out to be stable (attractive), but the (13,0) is weakly repulsive. The unrelaxed and relaxed structures are illustrated in Fig. 3. In the (13,0) SWCNT the optimized geometry of the nanowire is slightly distorted relative to the unrelaxed one (see the upper panel of Fig. 3). The average diameter of the nanotube increases from 10.33 Å to 11.04 Å, and the width of the wire shrinks from 7.37 to 7.26 Å. As far as the magnetism is concerned a striking change takes effect: we cannot stabilize the FM structure and a special AP ordering appears. The average magnetic moment of the interior iron atoms is opposite to that of the peripheral ones, which amounts to a qualitative reordering of the magnetic structure. The average magnetic moment of the carbon atoms is less than 0.1 μ_B. The magnetic moments and charges of the Fe atoms are shown in Table III. The nanowire encapsulated in the (15,0) SWCNT after relaxation may change its structure from hcp to bcc. Both situations are stable and their energies differ by 1 eV per unit cell, or 0.04 eV per Fe atom, favoring the bcc (001) structure. In that case the initial wire diameter of 7.47 Å stretches to 8.04 Å

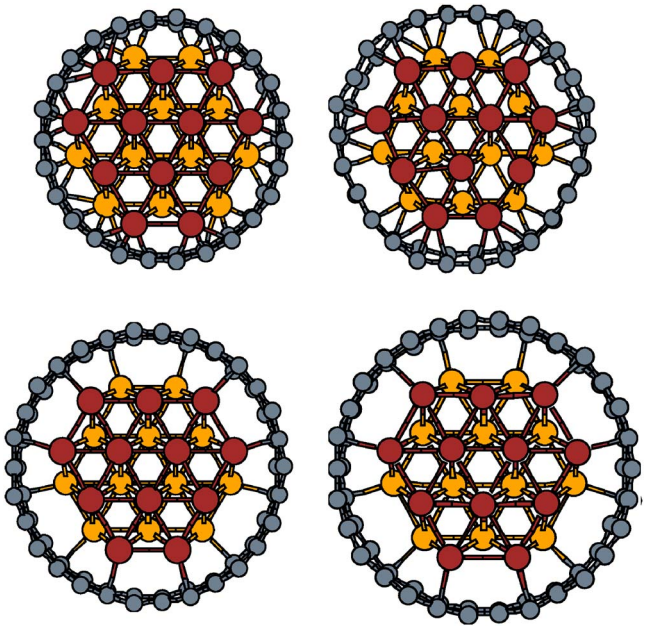

FIG. 3. (Color online) Iron hcp (0001) nanowire, with 12 Fe atoms per layer, encapsulated in a carbon nanotube system. The top illustrations correspond to the (13,0) SWCNT, and the bottom ones to the (15,0) nanotube. The unrelaxed configurations are shown on the left and relaxed configurations on the right. The atoms are represented in the same way as in Fig. 2.

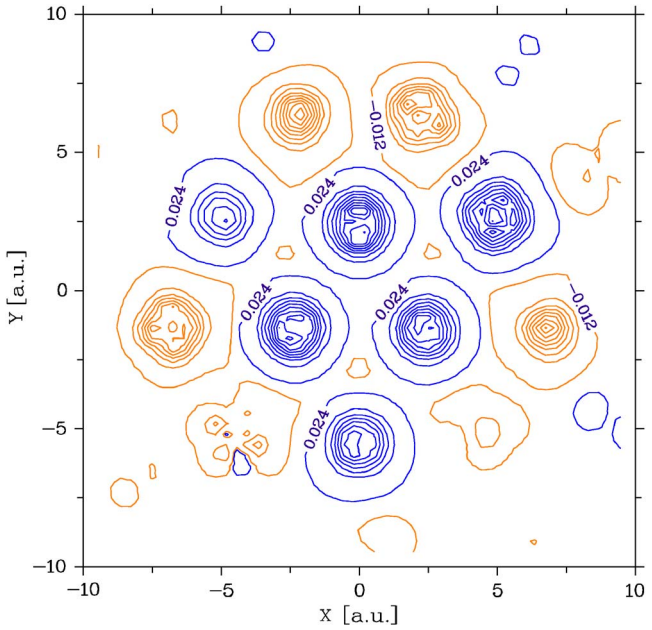

FIG. 4. (Color online) Isocurves of the difference between the spin up and the spin down charge densities for one layer of the 12 Fe-atom per layer wire encapsulated in a (13,0) carbon nanotube. The darker color represents a net spin up and the lighter color a net spin down charge. (a.u.) stands for atomic units.

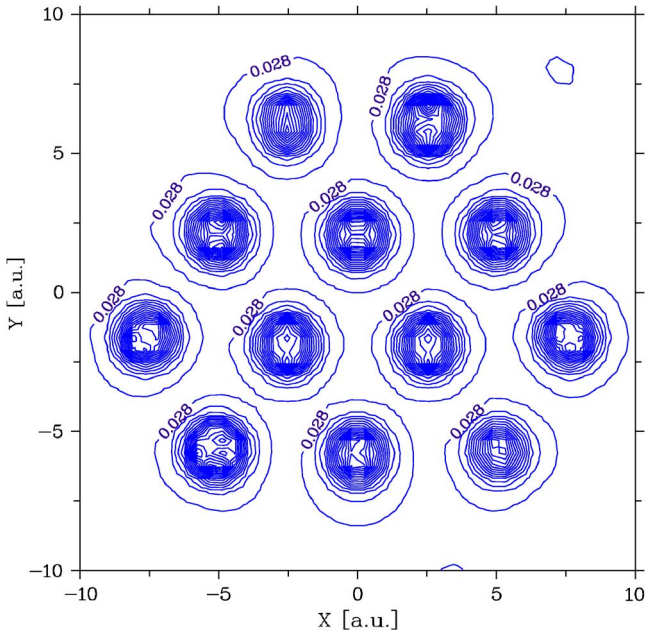

FIG. 5. (Color online) Isocurves of the difference between the spin up and the spin down charge densities for one layer of the 12 Fe-atoms per layer wire encapsulated in a (15,0) carbon nanotube. All the Fe atoms show a net spin up charge. (a.u.) stands for atomic units.

after relaxation and the nanotube also increases its diameter from 11.85 Å to about 12.2 Å. If the structure remains as hcp (0001) the change in the dimensions is much smaller (7.59 Å and 11.94 Å).

The isocurves of the spin density distribution for the 12-Fe per layer wire encapsulated in (13,0) and (15,0) SWCNT are shown in Figs. 4 and 5, where the darker (lighter) color represent the net spin up (down) charge. As mentioned before, in the more tightly encapsulated (13,0) nanowire the charge densities of the outermost iron atoms polarize opposite to the inner ones. Associated with this polarization is a charge transfer from the Fe to the C atoms as seen in Table III.

The average magnetic moment of the innermost iron atoms is $2.1\mu_B$, while for the outermost it is $-1.2\ \mu_B$. The situation is quite different for the wire encapsulated in the (15,0) SWCNT since all the iron atoms are polarized in the same direction, with almost the same charge, and also a negligible charge transfer. For the (15,0) SWCNT all the iron atoms have a magnetic moment of $\approx 2.6\mu_B$.

The densities of states of the relaxed structures for the 12-Fe atoms per layer wire encapsulated in (13,0) and (15,0) SWCNT, for the majority and minority bands, are shown in Fig. 6. The density of states at the Fermi level for the (15,0) SWCNT greatly differs for the spin up and the spin down bands. Although zig-zag carbon nanotubes $(n,0)$ can be semiconductors or metals according to the value of n, those filled with Fe are always metallic. The interesting parameter is the spin polarization of the electrons at the Fermi level. When the diameter of the nanotube is large, the spin polarization is also large, as for the bare nanowires. These systems could be of interest for the use in electron spin injection.

It also is interesting to compare the effect of encapsulating hcp (0001) nanowires (which are FM when freestanding) with hcp (0001) slabs (which are layered AF when freestanding). For this reason we computed the energies and magnetic configurations of a system built as a "sandwich," with two graphene layers on the "outside" and three iron layers, hcp like ordered (ABA), "inside." The lowest energy configuration corresponds to the A type iron atoms located on top of the nearest carbon atom of the graphene layer. The magnetic structure of the three iron layers is AP-like, that is up-down-up, for stable ABA configurations (attraction between the iron slab and the graphene layers). As we have seen, encapsulated iron nanowires are always FM unless the Fe atoms are very close to the C atoms, in which case AP order may appear. In fact, the case of a 12-Fe per layer wire inside a (13,0) SWCNT is only slightly repulsive, and thus one could expect that thicker wires could be attractive and with concentric layers ordered AP. It had been suggested by Prados *et al.*[5] that inside the CNT there may be a core of bcc iron surrounded by antiferromagnetic fcc iron, which seems similar to this situation. Also, this magnetic structure can be imagined as the "rolling up" of the previous slab along its axis.

C. Fe nanowires encapsulated in defective SWCNT

We have also considered nanowires encapsulated in defective SWCNT, hereafter denoted as dCNTs. Our purpose is to explore the structural and magnetic effects of vacancies or vacancy clusters, represented as abundant defects in carbon nanotubes. Also, to analyze the possibility that the inclusion of an excess of inserted iron may break the SWCNT or pre-

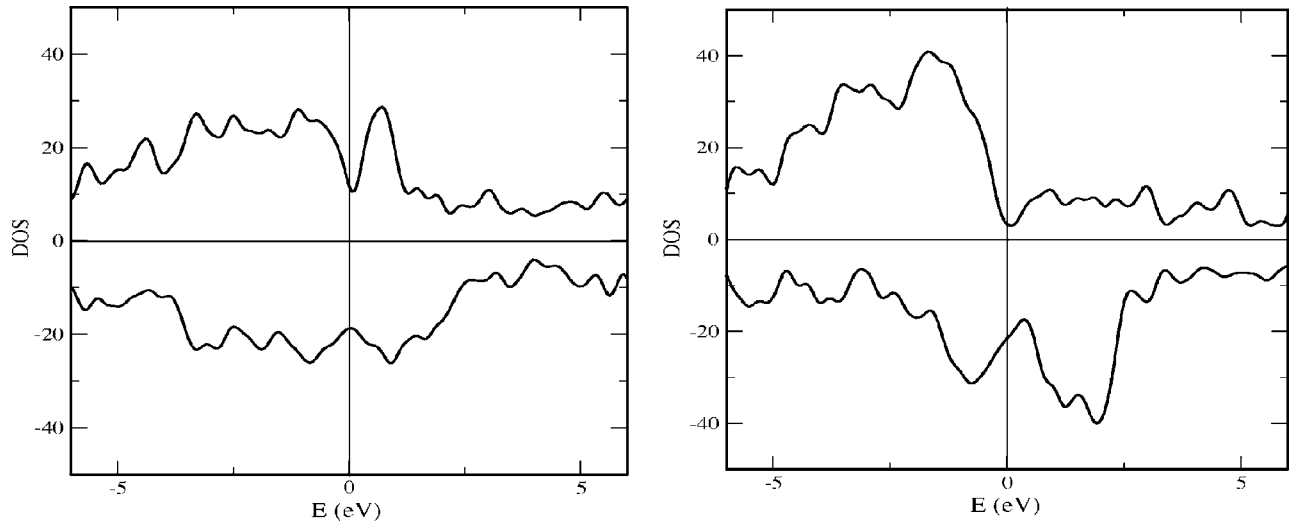

FIG. 6. Densities of states of wires with 12 Fe atoms per layer, encapsulated in a (13,0) nanotube (left) and in a (15,0) nanotube (right) for the majority (positive) and the minority (negative) spins. Notice the significant difference between majority and minority densities at the Fermi level for the nanowire in the (15,0) nanotube.

vent self-healing. Due to the size of the unit cell used in the present calculations the defects we studied remove a whole row of atoms along the nanotube. Although there is no experimental evidence for this type of defect we believe that the local structure and magnetic moments close to the vacant sites will, in general, be adequately described. Unfortunately not much experimental data on the structure of the most frequent defect is available, and in this respect we mention that large defects have been recently proposed to reconcile the discrepancy between experimental[36] and calculated[37,38] fracture strengths of unfilled carbon nanotubes. The type of defect studied here is illustrated in Fig. 7 and consists of removing 2 or 3 carbon atoms from the unit cell. The examples we show below remove 3 carbon atoms from the (11,0) SWCNT and 2 carbon atoms from the (12,0) one.

To create such a defect in the SWCNT has a large energy cost which can be estimated as $E_{\mathrm{dCNT}}-E_{\mathrm{CNT}}+N_{\mathrm{C}}E(\mathrm{C})$, where N_{C} is the number of C atoms that is removed [3 and 2 for the $d(11,0)$ and $d(12,0)$, respectively], and $E(\mathrm{C})$ is the energy of the C atom calculated in the same way as for the nanotube and the encapsulated system. The values we obtained are 32.7 eV and 20.5 eV for the $d(11,0)$ and $d(12,0)$, respectively. However, in fullerenes it was observed that C_2 molecules, instead of single C atoms, are generated. Thus, it is more realistic to reduce these values by 9.5 eV, the formation energy of C_2.

For the iron wire encapsulated in a defective nanotube we calculate the interaction energy as $E=E_{\mathrm{dCNT+Fe}}-E_{\mathrm{dCNT}}-E_{\mathrm{NW}}$. For the (11,0) nanotube the interaction energy is −7.3 eV, while for the (12,0) case it is −5.4 eV. We notice that in both cases this implies that these structures are more favorable than the same iron wire encapsulated in a perfect SWCNT. However, it is not easy to generate this type of defect in a nanotube due to the large energy required.

The magnetic moments of the carbon atoms in the bare defective SWCNT are negligible, except for some C atoms on the edge of the nanotube opening where $\mu_{\mathrm{at}}\approx 0.7\mu_B$, a behavior that is consistent with recent reports.[39,40] For the total magnetic moment of the (11,0) and (12,0) dCNT we obtain 0.8 and 0.0 μ_B per unit cell, respectively. It is worth mentioning that the (12,0) defective SWCNT "heals" the defect upon relaxation, by closing the gap between carbon atoms on opposite edges of the defect. The (11,0) dCNT+Fe instead remains open along the cut as illustrated in Fig. 7. These results are similar to those of fullerene molecules, that eject C_2 molecules and rebond when excited by laser radiation.

When these dCNT are filled with an Fe hcp (0001) NW with 6 atoms per layer all the magnetic moments change. For

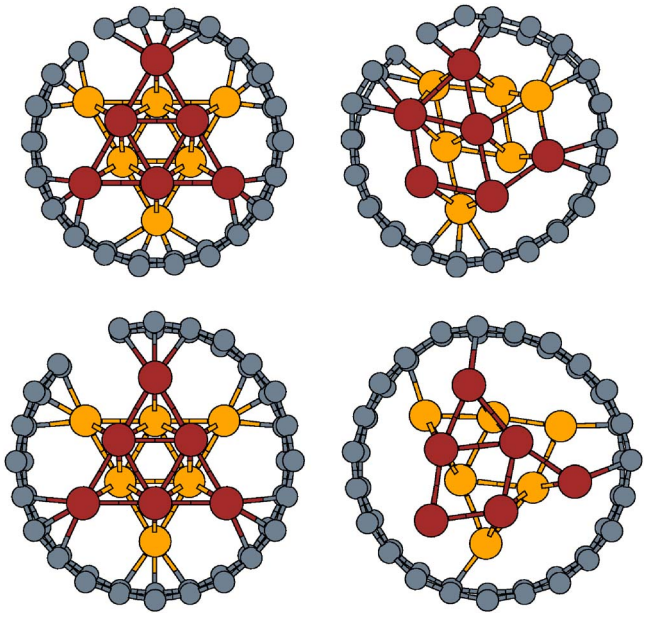

FIG. 7. (Color online) Iron hcp (0001) nanowire, with 6 atoms per layer, encapsulated in defective carbon (11,0) (upper panel) and (12,0) zig-zag (lower panel) nanotubes. The atoms are represented the same way as in Fig. 2. The left (right) illustration corresponds to the unrelaxed (relaxed) case.

the $d(11,0)$ case the moment of the C atom close to the defect decreases considerably and orders antiparallel to that of the nearest Fe atom, which is also very small, $1.3\mu_B$. However, the interior Fe atoms have moments of $2.8\mu_B$. For the $d(12,0)$ case the effect subsists but it is smaller, again the Fe atoms close to the defect have a smaller magnetic moment than the interior ones, $2.2\mu_B$ versus $2.8\mu_B$. It is interesting to compare this with the previous results for perfect SWCNT, where the magnetic moment of all the Fe atoms was the same. It is clear that defects in the nanotube structure influence the magnetic properties of the composite system.

IV. SUMMARY AND CONCLUSIONS

We have examined the properties of iron nanowires encapsulated in SWCNT, through the study of several specific examples. We started considering free standing iron nanowires to precisely determine the changes brought about by the Fe-C interaction. The Fe nanowire geometries we adopted consist of an increasing number of iron atoms per layer, and two layers per unit cell, arranged in hcp (0001) and bcc (011) structures repeated periodically parallel to the wire axis. In all cases the ferromagnetic structure was lower in energy, in spite of the fact that bulk hcp iron and hcp (0001) slabs are antiferromagnetic.

Next we computed the variations due to the encapsulation of nanowires with 6 and 12 Fe atoms per layer into zig-zag SWCNT of varying diameter, both with and without defects. In the small diameter SWCNT, where the iron wire fits very tightly, the encapsulated system is unstable and the iron may order AP. In these cases the magnetic moment of the Fe close to the C is small and there is a transfer of electrons from Fe to C. As one may expect, the repulsive interaction between the NW and the SWCNT, per Fe atom, is smaller for thicker wires and it may even change sign for the large diameter wires used experimentally. As the diameter of the CNT increases the internal and peripheral magnetic moments tend to equalize, the charge transfer tends to disappear and a binding energy between the wire and CNT appears. The maximum attractive interaction amounts to about 0.3 eV per Fe atom. If the diameter of the SWCNT is large the binding energy decreases, the Fe-C orbital hybridization is small and the magnetism of the system is almost equal to the free standing nanowire, peripheral Fe atoms having larger magnetic moments.

Single wall carbon nanotubes with a linear defect were also investigated. While the stability and energetics of the system is only slightly altered, the magnetization of the iron atoms close to the defect are substantially reduced.

The fact that the AP and FM arrangements, especially in the case of tight encapsulation, have energies that differ only slightly points to their likely coexistence in real systems at finite temperatures. Thus, this may constitute an explanation for the observation of the exchange bias phenomenon in some systems that has recently been reported.[5,6]

ACKNOWLEDGMENTS

This work was supported by the Fondo Nacional de Investigaciones Científicas y Tecnológicas (FONDECYT, Chile) under Grants Nos. 1030957 (M.K.) and 1040356 (R.R.) and by MECESUP (G.G.).

[1] M. Monthioux, Carbon **40**, 1809 (2002).
[2] K. Svensson, H. Olin, and E. Olsson, Phys. Rev. Lett. **93**, 145901 (2004).
[3] N. Y. Jin-Phillipp and M. Ruhle, Phys. Rev. B **70**, 245421 (2004).
[4] M. Weissmann, G. García, M. Kiwi, and R. Ramírez, Phys. Rev. B **70**, 201401(R) (2004).
[5] C. Prados, P. Crespo, J. M. Gonzalez, A. Hernando, J. F. Marco, R. Gancedo, N. Grobert, M. Terrones, R. M. Walton, and H. W. Kroto, Phys. Rev. B **65**, 113405 (2002).
[6] S. Karmakar, S. M. Sharma, M. D. Mukadam, S. M. Yusuf, and A. K. Sood, J. Appl. Phys. **97**, 054306 (2005).
[7] M. S. Ferreira and S. Sanvito, J. Magn. Magn. Mater. **290-291**, 286 (2005).
[8] N. Demoncy, O. Stéphan, N. Brun, C. Colliex, A. Loiseaux, and H. Pascard, Eur. Phys. J. B **4**, 147 (1998).
[9] J. B. Wang, X. Z. Zhou, Q. F. Liu, D. S. Xue, F. S. Li, B. Li, H. P. Kunkel, and G. Williams, Nanotechnology **15**, 485 (2004).
[10] G. Bilalbegović, Vacuum **71**, 165 (2003).
[11] C.-K. Yang, Appl. Phys. Lett. **85**, 2923 (2004).
[12] S. Karmakar, S. M. Sharma, P. V. Teredesai, and A. K. Sood, Phys. Rev. B **69**, 165414 (2004).
[13] T. Muhl, D. Elefant, A. Graff, R. Kozhuharova, A. Leonhardt, I. Monch, M. Ritschel, P. Simon, S. Groudeva-Zotova, and C. M. Schneider, J. Appl. Phys. **93**, 7894 (2003).
[14] B. C. Satishkumara, A. Govindaraja, P. V. Vanithaa, A. K. Raychaudhuric, and C. N. R. Rao, Chem. Phys. Lett. **362**, 301 (2002).
[15] C.-K. Yang, J. Zhao, and J. P. Lu, Phys. Rev. Lett. **90**, 257203 (2003).
[16] Y. Yagi, T. M. Briere, M. H. F. Sluiter, V. Kumar, A. A. Farajian, and Y. Kawazoe, Phys. Rev. B **69**, 075414 (2004).
[17] S. B. Fagan, R. Mota, A. J. R. da Silva, and A. Fazzio, Phys. Rev. B **67**, 205414 (2003).
[18] Y.-J. Kang, J. Choi, C.-Y. Moon, and K. J. Chang, Phys. Rev. B **71**, 115441 (2005).
[19] T. Nautiyal, T. H. Rho, and K. S. Kim, Phys. Rev. B **69**, 193404 (2004).
[20] J. Nogués and I. K. Schuller, J. Magn. Magn. Mater. **192**, 203 (1999).
[21] M. Kiwi, J. Magn. Magn. Mater. **234**, 584 (2001).
[22] B. Dieny, V. S. Speriosu, S. Metin, S. S. P. Parkin, B. A. Gurney, P. Baumgart, and D. R. Wilhoit, J. Appl. Phys. **69**, 4774 (1991).
[23] B. Dieny, V. S. Speriosu, S. S. P. Parkin, B. A. Gurney, D. R. Wilhoit, and D. Mauri, Phys. Rev. B **43**, R1297 (1991).
[24] P. Ordejón, E. Artacho, and J. M. Soler, Phys. Rev. B **53**, R10441 (1996).
[25] J. M. Soler, E. Artacho, J. D. Gale, A. García, J. Junquera, P. Ordejón, and D. Sánchez-Portal, J. Phys.: Condens. Matter **14**,

2745 (2002).
[26] J. M. Soler, M. R. Beltran, K. Michaelian, I. L. Garzon, P. Ordejón, D. Sánchez-Portal, and E. Artacho, Phys. Rev. B **61**, 5771 (2000).
[27] P. Blaha, K. Schwarz, G. K. H. Madsen, D. Kvasnicka, and J. Luitz, *An Augmented Plane Wave + Local Orbitals Program for Calculating Crystal Properties* (Karlheinz Schwarz, Techn. Universität Wien, Austria, 2001), isbn 3-9501031-1-2.
[28] J. P. Perdew and A. Zunger, Phys. Rev. B **23**, 5048 (1981).
[29] J. P. Perdew, K. Burke, and M. Ernzerhof, Phys. Rev. Lett. **77**, 3865 (1996).
[30] J. P. Perdew, K. Burke, and M. Ernzerhoff, J. Chem. Phys. **105**, 9982 (1996).
[31] P. Hohenberg and W. Kohn, Phys. Rev. **136**, B864 (1964).
[32] W. Kohn, Rev. Mod. Phys. **71**, 1253 (1999).
[33] C. C. Fu, F. Willaime, and P. Ordejon, Phys. Rev. Lett. **92**, 175503 (2004).
[34] C. Fu, J. D. Torre, F. Willaime, J. L. Bocquet, and A. Barbu, Nat. Mater. **4**, 68 (2005).
[35] R. Saito, G. Dreselhaus, and M. S. Dreselhaus, *Physical Properties of Carbon Nanotubes* (Imperial College, London, 1998).
[36] M.-F. Yu, O. Lourie, M. J. Dyer, K. Moloni, T. F. Kelly, and R. S. Ruoff, Science **287**, 637 (2000).
[37] S. Zhang, S. L. Mielke, R. Khare, D. Troya, R. S. Ruoff, G. C. Schatz, and T. Belytschko, Phys. Rev. B **71**, 115403 (2005).
[38] A. V. Krasheninnikov, K. Nordlund, and J. Keinonen, Phys. Rev. B **65**, 165423 (2002).
[39] Y.-H. Kim, J. Choi, K. J. Chang, and D. Tománek, Phys. Rev. B **68**, 125420 (2003).
[40] P. O. Lehtinen, A. S. Foster, Y. Ma, A. V. Krasheninnikov, and R. M. Nieminen, Phys. Rev. Lett. **93**, 187202 (2004).